35th Annual International Conference of the IEEE EMBS
Osaka, Japan, 3 - 7 July, 2013

A simple microfluidic gradient generator with a soft-lithographically prototyped, high-aspect-ratio, ~2 μm wide microchannel*

Tomohisa Ogawa, Nirai Matsunaga, Saori Inomata, Masato Tanaka and Nobuyuki Futai

Abstract— **We have developed a cast microfluidic chip that contains a thin (~2 μm wide) microchannel that is smoothly connected to thick microfluidics. The thin line features having high aspect ratio for a low-cost photolithography in which an emulsion photomask was used (1:1 ~ 1:3) were fabricated by exposing SU-8 photoresist to diffused 185 nm UV light emitted by a low-cost ozone lamp from the backside of the substrate to ensure sufficient crosslinking of small regions of the SU-8 photoresist. An H-shaped microfluidic configuration was used, in which the thin channel maintained constant diffusion fronts beyond purely static diffusion. We also demonstrated the long-term effects of a gradient of nerve growth factor on axon elongation by primary neurons cultured in the micro channel.**

I. Introduction

Cells naturally respond to soluble factor gradients through processes such as chemotaxis, gradient-dependent differentiation, and axon guidance. The generation of concentration gradients in media covering cells seeded in microfluidic devices is a useful tool for investigating such processes[1]. In addition, the microfluidic approach to gradient generation has higher throughput and is more efficient than gradient generation in traditional culture systems[2].

Challenges remain, however, in designing microfluidic gradient generators that are simple to fabricate and convenient to use. Such devices are still underused because microfluidic, or lab-on-a-chip, technologies lack technical simplicity[3]. They often require systems for complex microfabrication and/or microfluidic control techniques that many end users find difficult to adopt. Another scientific difficulty arises in calibrating the gradient, i.e. in estimating or predicting the spatiotemporal concentration profile in a chip that has a complex microfluidic configuration both in terms of channel layout and external equipment.

We have developed a cast microfluidic chip that contains a thin (width of ~2 μm at the base; the aspect ratio ranging 1:1 ~ 1:3) microchannel that is smoothly connected to thicker microfluidics. The thin channel has high flow resistance and supports diffusion-based gradient generation and easy handling, including priming. The end of the thin channel can be considered as a point source that facilitates the prediction and analysis of the spatiotemporal concentration gradient generated. In addition, we note that our method of mold fabrication for casting should also be simple enough for end users to prepare.

We also developed a fabrication method for the SU-8 photoresist channel mold with mixed cross-sectional dimensions patterned only by conventional photolithography. This method was based on a soft lithographic rapid prototyping of SU-8 features at 8 μm resolution using cost-effective photoplotted (emulsion) masks. The limitation in resolution of this simple rapid prototyping method comes from the resolution/transparency of the photoplotted masks [4] and insufficient crosslinking of SU-8 photoresist by UV light through an aperture smaller than 8 μm. We have successfully fabricated SU-8 line features defined by an emulsion glass mask with widths of ~2 μm at the base. The line features had high aspect ratio for a low-cost UV lithography by using diffused 185 nm UV emitted from a low-cost ozone lamp as the light source for UV exposure. The UV light was exposed from the backside of the substrate to ensure sufficient crosslinking of small regions of the SU-8 photoresist layer.

II. Materials and Methods

A. Design of the Microfluidic Chip

The microfluidic gradient generator chip we developed and its fluidic configuration are shown in Fig 1. The chip consists of a glass-bottom dish and a circular slab made of poly(dimethylsiloxane) (PDMS) with microfluidic channel features and two inlet/outlet pairs (Fig.1A). The microchannels (Fig.1B) include one thin channel with smooth sidewalls (1.5 μm wide × 1.5 μm high × 40 μm long), and thick channels (200 μm wide × 30 μm high) that bifurcate from each end of the thin channel so that the fluidic configuration is H-shaped (Fig.1C). The right-hand side of the H-shape is mainly used for introducing cells and allows for easy cell loading under low shear stress. The left-hand side of the H-shape is used for introducing test substances, and the channel height decreases at the branch point to ensure complete liquid exchange.

B. Fabrication of Microfluidic Chip

The fabrication processes is illustrated in Fig 2. The combination of backside exposure of SU-8 photoresist[5] and exposure of short-wavelength (185 nm) UV was used for the first SU-8 patterning. First, a 50 nm Cr film was deposited on a synthetic fused silica glass wafer (t0.3 mm) by sputtering. The wafer was then coated with a 1 μm thick layer of positive photoresist (FPPR-P10, Fuji Chemicals Industrial) by

*Research supported by a grant of Strategic Research Foundation Grant-aided Project for Private Universities from Ministry of Education, Culture, Sport, Science, and Technology (MEXT), 2008-2012 (S0801023).

T. Ogawa is with the School of Medical and Dental Sciences, Tokyo Medical and Dental University, Tokyo, 113-8510 Japan.

N. Matsunaga, S. Inomata and M. Tanaka are with the School of Science and Engineering, Tokyo Denki University, Saitama, 350-0394 Japan.

N. Futai is with Dept. Mechanical Engineering, Shibaura Institute of Technology, Tokyo, 135-8548 Japan (corresponding author to provide phone: 03-5859-8008; fax: 03-5859-8001; e-mail: futai@shibaura-it.ac.jp).

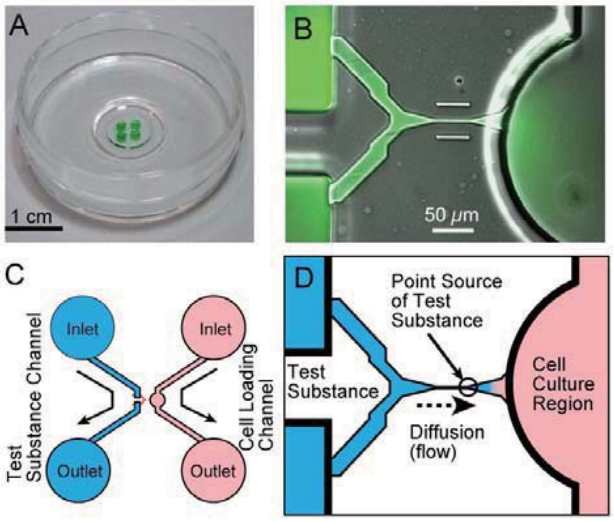

Figure 1. Microfluidic static gradient generator with a single high-flow-resistance microchannel. A) Assembled microfluidic chip: a poly(dimethylsiloxane) (PDMS) circular slab with microchannel features bonded on a glass-bottom dish. B) Micrograph of the microfluidic channels at the center of the chip. Fluorescence from the solution introduced to the channels is overlaid on the phase contrast image. A gradient of fluorescence was generated in the rounded cell culture region of the channel on the right. C) Channel configuration: asymmetrical H-shaped channel with a thin channel at the center. D) Illustration of gradient generation on the chip. The exit of the thin channel acts as a point source for a test substance, creating a concentration gradient into the cell culture region.

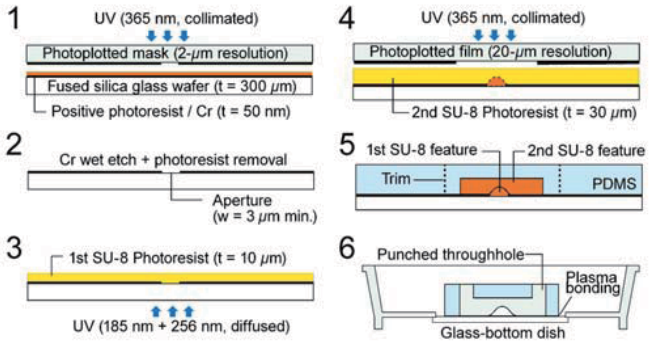

Figure 2. Fabrication process of microfluidic chip with thin and thick mixed-height microchannels. The first four steps illustrate the fabrication of a channel mold, and the remaining steps describe the casting and assembly of the chip. Process overview: 1) patterning of positive photoresist onto sputtered Cr film on a fused silica glass wafer, 2) wet etching of Cr to make the apertures that serve as a photomask, 3) patterning of thin channel features (2–20 μm width at the base) by high-energy UV exposure of SU-8 photoresist through the Cr apertures, 4) patterning of another SU-8 layer into the thick channel features (~200 μm wide) by conventional photolithography, 5) casting of PDMS using the channel features as a mold, and 6) bonding of the cast PDMS onto a glass-bottom dish.

spin-coating at 5,000 rpm. The photoresist layer was exposed to collimated UV light (10 mW/cm^2 @ 365 nm) for 5 s through an emulsion glass photomask (2 μm resolution, Shineisha) and was then developed. The exposed Cr film was wet etched in a solution containing 17 wt% $(NH_4)_2Ce(NO_3)_6$ and 7 wt% NH_4NO_3 in water. Photoresist was then removed using acetone and the substrate was cleaned using a detergent.

Next, the SU-8 photoresist layer on the patterned Cr film was exposed to UV from the backside to form thin channel features. A negative photoresist (SU-8 3005) was spun at 4,500 rpm for 30 s to form a layer with a thickness range of 8–10 μm and was dried at 95 °C for 10 min. The SU-8 layer was then exposed to 185 nm and 254 nm UV from a 4W low-pressure mercury vapor lamp (ozone lamp). The UV power was measured as 0.2 mW/cm^2 @ 185 nm. The exposure time was controlled by an electronic shutter so that the exposure dose ranged from 0.1–1.0 mJ/cm^2.

Following the backside exposure, a thick SU-8 layer was patterned using conventional methods. A 30 μm thick negative photoresist layer (SU-8 3035) was coated by spinning at 3,000 rpm for 30 s, dried, and exposed to the collimated 365 nm UV with a dose of 300 mJ/cm^2 through an emulsion glass photomask (10 μm resolution, Topic-dic) aligned to the first SU-8 layer using a 3-axis mechanical stage. Both exposed SU-8 layers were post-exposure baked at 95 °C for 10 min and were developed.

Finally, the SU-8 features were transferred to a PDMS circular slab, which was then bonded to the bottom of a glass bottom dish for cell culture. A PDMS prepolymer (KE106, Shin-etsu) was poured onto the SU-8-pattened surface to make a 1 mm thick layer, cured at 110 °C for 15 min, and demolded by peeling. An 8 mm diameter circular slab containing the microfluidic upper channel was punched from the peeled PDMS, and four 2 mm diameter holes (Fig. 1C) were punched in the circular slab. The punched PDMS slab was bonded to a 35 mm diameter glass-bottom dish after air plasma treatment at 20 Pa for 30 s.

C. Measurement of Channel Dimensions

Cr patterns on the glass wafers were photographed by a CCD camera (DMK41AU02, The Imaging Source) on an optical microscope (OPTIPHOT-66, Nikon) and were analyzed using image processing software (ImageJ v1.4). The texture and height images of the surface of PDMS slabs with thin channel upper features were acquired by a laser confocal microscope (OLS3500, Olympus) and analyzed using height field and image analysis software (Gwyddion v2.30).

C. Evaluation of Diffusion on Chip

An assembled chip was primed by introducing deionized water to the inlets/outlets. The height of each droplet was adjusted to approximately 0.5 mm to apply Laplace pressure of ~180 Pa. To load the thin channel with fluorescence, the water droplet at the inlet to the Test Substance Channel (Fig. 1C) was replaced with 0.2 wt% sodium fluorescein solution. Next, the other water droplets were suctioned to create a concave height of ~0.5 mm. The three concave water surfaces generated flows that introduced fluorescein into the thin channel because of negative Laplace pressure. Finally, the inlets/outlets were positively pressurized again as described above when necessary. A CCD camera (ORCA-R2, Hamamatsu) on an inverted fluorescent microscope (TE2000U, Nikon) was used for fluorescence microscopy with time-lapse recording.

For the axon elongation experiment, primary dorsal root ganglion (DRG) cells were introduced to the chip. The DRG

cells were freshly isolated from E7 chick embryos by dissection, and were dissociated into DRG cells using 0.25% trypsin. The channels were coated with a solution of 1 wt% poly-D-lysine and filled with DMEM/F12 medium with Insulin/Transferrin/Selenium (ITS) supplement. The DRG cells were seeded from the inlet of cells (Fig. 1C) and attached near the node. 50 ng/ml nerve growth factor in DMEM/F12 was introduced to the inlet of the Test Substance Channel, and the device was then incubated at 37 °C and 5% CO_2 for 16 h. The cells were observed on the same system for fluorescence microscopy as described above.

III. Results and Discussion

A. *Size of the microfluidic channels*

The dependence of the size of the PDMS microfluidic channel features on the exposure dose at 185 nm during the fabrication of the SU-8 mold is shown in Fig 3. Because the aperture that defines the area of the SU-8 features was widened at both ends, the widths of the resulting microfluidic channels were also increased. Here we note that the height of the channel was also increased as the aperture width increased. As the aperture width exceeded ~7 µm, the height remained steady at the saturation height, which depended on the exposure dose (Fig.3B). The limited penetration depth of SU-8 photoresist layer for 185 nm UV may determine the saturation height. The heights of the thin channel defined by the 3 µm wide aperture were slightly lower than the saturation value, suggesting the small aperture also restricted the channel height. However, the exposure dose at 185 nm appears to be the dominant factor in determining the channel height.

The channel width thickened slightly from the nominal aperture width as the exposure dose was increased (Fig. 3C). We compared the exposure dose to the ratio: (channel width – aperture width) / aperture width. For low exposure doses (e.g. 0.1 mJ/cm^2), this ratio was negative, suggesting that the effect of the limited penetration of 185 nm UV to SU-8 was stronger than the lateral crosslinking due to scattering and diffusion of light. The thickening of channel width with exposure dose was small, particularly at the exposure dose of 0.15–0.2 mJ/cm^2. Even at larger exposure doses, the magnitude change in width was within 4 µm. Thus, the dependence of effective channel width on the exposure dose was not very pronounced compared with that of channel height.

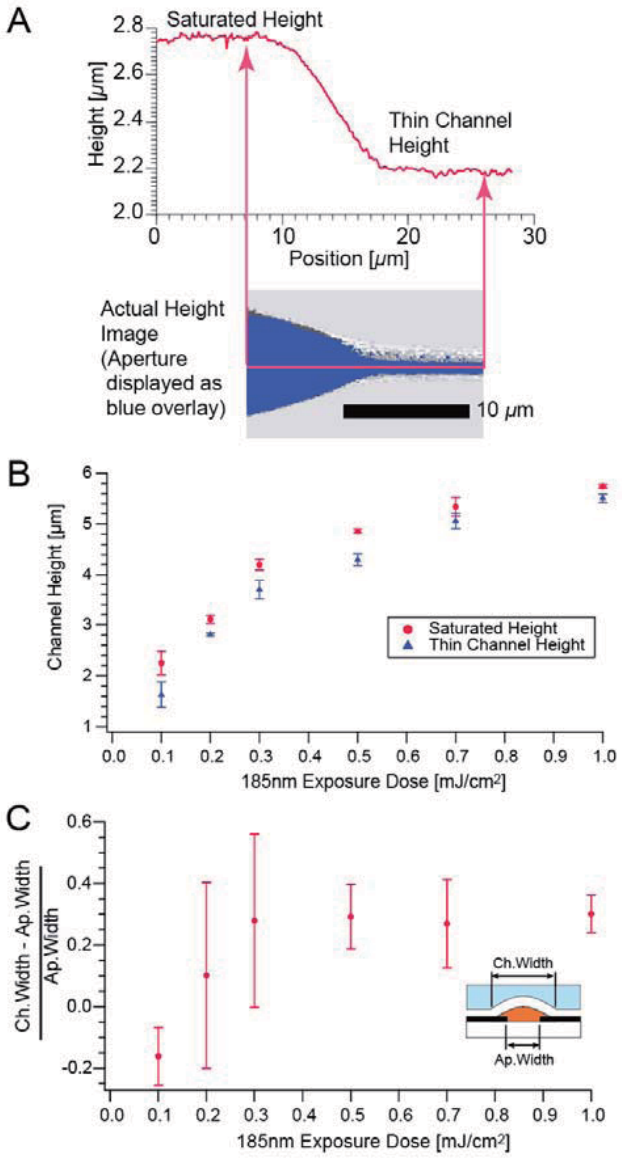

Figure 3. The size of PDMS microfluidic features transferred from patterned SU-8 photoresist is influenced by factors in photolithography: the exposure dose and the width of Cr apertures. A) A laser confocal height image of a typical thin channel with widening ends. The exposure dose at 185 nm was 0.3 mJ/cm^2. The height of the feature was saturated even if apertures wider than 7 µm were used. B) The thin channel height and saturated height as functions of exposure dose @ 185 nm (mean ± *SD*, $N = 3$–6). C) The ratio of the width increment (channel width – aperture width) to the aperture width plotted as a function of exposure dose @ 185 nm (mean ± *SD*, $N = 3$).

B. *Gradient generation*

We were able to control the concentration gradient of test substances inside or at the exit of the thin microchannel by adjusting the pressures at the inlet/outlet, as shown in Fig 4. Gradients were generated (Figs. 4A and B) for an example fluorophore (sodium fluorescein) after a drop of fluorophore solution was applied to the Test Substances Channel inlet (Fig.1C) to apply Laplace pressure at the inlet. The gradient of fluorophore remained constant in the thin channel (Fig. 4A) over a long period of time (600 s) by applying positive Laplace pressure also at the Cell Loading Channel inlet/outlet (Fig.1C). The movement of the diffusion front (Fig.4A) over 600 s was estimated to be less than 5 µm. Conversely, applying negative Laplace pressure at the Cell Loading Channel inlet/outlet rapidly pushed fluorophore to the exit of the thin channel (Fig. 4B), eventually generating a gradient at the cell culture region (Fig.1B). The transit time of the diffusion front across the 40 µm thin channel length, measured from the intensity profile, was approximately 5.5 s.

The diffusion behavior observed in the above two cases were different from the model of one-dimensional static diffusion from a continuous point source:

$$C(x,t) = C_0 \,\mathrm{erfc}\left[\frac{x}{2\sqrt{Dt}}\right]$$

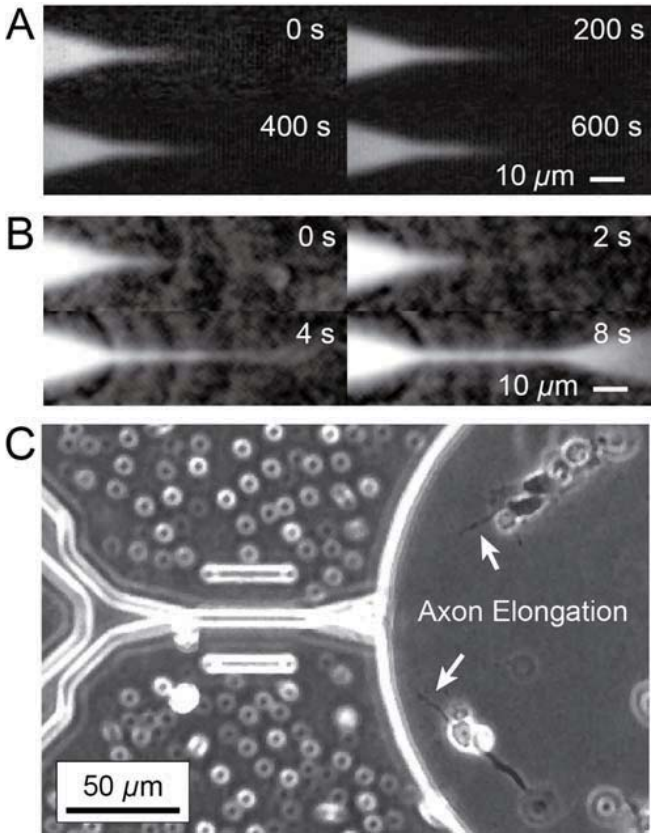

Figure 4. Concentration gradients generated on the H-shaped microfluidic configuration with the thin channel at the center. A) Time evolution of the diffusion front of sodium fluorescein initially introduced to one end of the thin channel. Both ends of the thin channel were Laplace pressurized at the inlets/outlets after introducing the fluorophore. B) Time evolution similar to A), but with different pressurizing. In this case, the ends of the thin channel were not re-pressurized after introducing the fluorophore. C) Axon elongation of primary nerve (dorsal root ganglion: DRG) cells from chick embryo after 16 h in culture on the chip. The axons are directed toward the end of the thin channel that supplies nerve growth factor (NGF).

where $C(x,t)$ is the concentration at position x and time t, C_0 the concentration at the point source, and D the diffusion coefficient (371 $\mu m^2/s$ for sodium fluorescein in water at 20 °C). When we defined the concentration at the diffusion front as $0.9C_0$, the predicted values for the diffusion front movement and transit time were 83.9 μm over 600 s and 136.5 s for the 40 μm length. Our results indicate <5 μm front movement over 600 s and a 40 μm length transit time of ~5.5 s, both significantly smaller than the predictions. These results show that the developed microfluidic configuration can generate or maintain concentrations beyond purely static diffusion. When the ends of the thin channel were not re-pressurized (Fig.4B), it is reasonable to assume that there was a pressure-driven flow in the thin channel due to the negative pressures at the cell inlet/outlet (Fig.4B) that decreases transit time. However, after pressurizing the inlet/outlets (Fig.4A), stable gradients were typically observed over a wide range of positive pressures. The high resistance and high surface/volume ratio of the thin channel may explain this tendency of limited flow velocity (opposite to the direction of diffusion) within a certain range that can successfully slow down the progression of the diffusion front.

C. Guided Axon Elongation

Using a slow movement diffusion front (Fig.4A), we examined the long-term effect of NGF on primary DRG neurons cultured in the microfluidic channel. NGF is known to contribute to axon elongation, guidance and survival, and we demonstrated axon elongation towards the exit of the thin channel (Fig.4C), which can be considered as the point source of NGF. This result shows that a sharp gradient of NGF was sufficient to define the direction of axon elongation and was maintained for a long period (~16 h) because of minimal diffusion and the small size of the thin channel. Compared with a previous microfluidic axon separation device [6], this configuration more easily enables end users to track the combination of single cells and their axons and to observe the directional response of axons using asymmetrical gradients. We did not observe axon separation (an axon passing through the thin channel). However, increasing the seeding cell density and adjusting the initial concentration of NGF at the point source may allow us to promote axon separation within this single thin channel chip.

IV. Conclusion

We have demonstrated the fabrication of microfluidic channels with various cross-sectional sizes, ranging from 2–6000 μm^2 using a simple soft lithographic method. 185 nm diffused UV from a commercially available ozone lamp successfully patterned SU-8 photoresist into thin (1.5 μm × 1.5 μm) microfluidic channel features at low cost. These thin, H-shaped channels in PDMS microfluidic chips successfully generated visible local gradients because of slow diffusion controlled by Laplace pressures. Since the chip fabrication and fluidic control are simple enough to be implemented by non-experts, this mixed-height microfluidic chip could provide opportunities for a wide range of biomedical experiments and diagnostics investigating cellular response in microscale physicochemical systems.

Acknowledgment

We thank Dr. Tomofumi Ukai and the Bio Nano Electronics Research Centre of Toyo University for the height field measurement using laser confocal microscopy.

References

[1] B. G. Chung and J. Choo, "Microfluidic gradient platforms for controlling cellular behavior," *Electrophoresis,* vol. 31, pp. 3014-27, Sep 2010.

[2] D. B. Weibel and G. M. Whitesides, "Applications of microfluidics in chemical biology," *Curr Opin Chem Biol,* vol. 10, pp. 584-591, 2006.

[3] G. M. Whitesides, "Cool, or simple and cheap? Why not both?," *Lab Chip,* vol. 13, pp. 11-13, 2013.

[4] V. Linder, H. Wu, X. Jiang, and G. M. Whitesides, "Rapid prototyping of 2D structures with feature sizes larger than 8 microm," *Anal. Chem.,* vol. 75, pp. 2522-7, May 15 2003.

[5] N. Futai, W. Gu, and S. Takayama, "Rapid Prototyping of Microstructures with Bell-Shaped Cross-Sections and Its Application to Deformation-Based Microfluidic Valves," *Adv Mater,* vol. 16, pp. 1320-1323, 2004.

[6] J. W. Park, B. Vahidi, A. M. Taylor, S. W. Rhee, and N. L. Jeon, "Microfluidic culture platform for neuroscience research," *Nat. Protoc.,* vol. 1, pp. 2128-36, 2006.